Numerical Solution of Electromagnetic Integral Equations by the Meshfree Collocation Method

B. Honarbakhsh[1], A. Tavakoli[1, 2]

[1]Department of Electrical Engineering
[2]Institute of Communications Technology and Applied Electromagnetics
Amirkabir University of Technology (Tehran Polytechnic), Tehran, IRAN
b_honarbakhsh@aut.ac.ir, tavakoli@aut.ac.ir

Abstract ― This paper presents guidelines for mesh free numerical solution of electromagnetic integral equations. Both static and dynamic problems are considered, including the EFIE and the MPIE for dynamic case. Different choices of the kind of meshfree method, shape functions and their parameters are studied and proper choices are suggested by logical deduction, experience or previous reports. The final configuration is applied to classical problems in one and two dimensions such as electric charge (density) and electric current (density) distributions over a line and flat plates, respectively. The method is validated by convergence analysis and is compared with MoM. In addition, suggestions are made for bypassing numerical integrations that make the construction of the coefficient matrix integration free.

Index Terms ― collocation, EFIE, integral equation, meshfree, MPIE.

I. INTRODUCTION

Although there exist an extensive work on numerical solution of partial differential equations (PDEs) by meshfree methods (MFMs) [1]-[19], at present, volume of studies regarding integral equations (IEs) is negligible [20]-[23].

Meshless methods have four important advantages with respect to their mesh-based counterparts. First, they remove the need to a mesh generator, which requires a considerable CPU time especially for volumetric formulations. Second, the refinement process is extremely simpler. Third, the extreme capabilities of meshless shape functions in data fitting, leads to smaller matrices. Finally, since meshless shape functions usually have high order of continuity, differentiation and post processing are not of a concern.

IE solvers are of high importance in computational electromagnetics (CEM) and possess valuable properties. By the IE-based formulation, the discretization reduces only to the body under study. In contrast, when dealing with PDE solvers, the space surrounding the object should also be discretized; leading to additional memory and computational cost. IEs, also, remove the need for absorbing boundary condition (ABC) which is a bottleneck in numerical methods. Moreover, when dealing with practical problems ABCs are never precise.

EM IE solvers shortcut the above difficulties utilizing Green's function that is known for several practical situations; e.g., free space, half space and multilayer media [24]. Many realistic problems can be formulated by the aforementioned Green's functions including electromagnetic scattering, radar cross section (RCS), ground penetrating radars (GPR), microstrip antennas, planar microwave components, and lightning. The traditional numerical method for solving EM IEs is the method of moments (MoM) [25]-[27]. This method is mesh-based and uses simple expansion functions for approximating the unknown field variable and, in contrast to PDE solvers, leads to small but dense matrices.

The primary motivation of this work was extending the application domain of MFMs to IEs appearing in electrical engineering. Furthermore, since many practical problems are well formulated by hybridizing PDEs with IEs [28], [29] and noting that MFMs are powerful tools for solving

Submitted On: March 7, 2012
Accepted On: May 22, 2012

PDEs, the need for such researches becomes more comprehensible. In fact, the core ideas of this work are previously applied to such problems [30].

As a brief review on currently published works on meshfree solution of IEs, in [20] a 1D MPIE is solved over a thin straight wire by the Galerkin method and *moving least square* (MLS) shape functions as expansion functions. The work does not offer a justification for using the Galerkin type and MLS functions. Furthermore, the numerical integration strategy is not reported. Generalization of the method to more than 1D seems to be extremely time consuming and thus impractical. The major contribution of [21] is the error analysis of meshless collocation solution of the second kind Fredholm and Volterra IEs based on MLS shape functions. The given examples are abstract and of mathematical interest. Additionally, a justification for MLS method is not provided.

In [22], the CFIE is solved by meshless collocation method for bodies with cylindrical symmetry, at normal incidence. In such cases, the differential part of the IE is omitted, which considerably simplified the numerical solution. Moreover, the improved MLS (IMLS) method is used for shape function generation which is justified only in comparison with the MLS method. Finally, Hallen's IE that corresponds to a straight linear antenna is solved in [23] by the meshless collocation method utilizing *radial bases functions* (RBFs). The use of RBFs is justified based on their powerful fitting capability. This property is also present in the MLS shape functions. Therefore, the rationalization does not exclude other shape functions.

In this paper, both static and dynamic EM IEs are considered, including the EFIE and the MPIE in the case of dynamic cases. In addition, different choices of the kind of meshfree method, shape functions and their parameters are studied and proper choices are suggested by logical deduction, experience or previous reports. Noting the intrinsic complexity of meshfree shape functions that makes their evaluation time-consuming, suggestions are made to bypass numerical integrations for a specific arrangement of equidistant node arrangement. Theoretically, the idea of bypassing numerical integrations could be extended to arbitrary node distributions and is currently under investigation. Even though, the approach is general, only regular node arrangements are considered here.

II. MATHEMATICAL STATEMENT OF THE PROBLEM

In this paper, we have restricted the formulation to classical EM problems governing PECs in one and two dimensions. The guidelines throughout the paper are general.

The IEs considered in this work are Fredholm integral/integro-differential equations of the first kind, which all could be *equivalently* expressed by the following mathematical statement:

$$\begin{cases} e = O_D(y), \text{ over } \Omega \\ y = O_I(f) \\ O_I(f) = G * f \\ O_B(f) = 0, \text{ over } \partial\Omega \end{cases} . \tag{1}$$

where:

$$\begin{cases} e: \text{ excitation} \\ f: \text{ field variable} \\ G: \text{ Green's function} \\ O_D: \text{ differential operator} \\ O_I: \text{ integral operator} \\ O_B: \text{ Dirichlet boundary condition operator} \\ \Omega: \text{ problem domian} \\ \partial\Omega: \text{ problem boundary} \\ *: \text{ linear convolution} \end{cases} . \tag{2}$$

It is worth mentioning that (1) is, in general, a set of vector valued equations. In addition, the presence of O_B is problem dependent and O_D may be simplified to a multiplicative scalar.

III. A BRIEF INTRODUCTION TO MESHLESS SHAPE FUNCTIONS

In meshfree community, the expansion functions are called *shape functions*, and fall into two main categories; *approximants* and *interpolants*. We briefly introduce these types and some of their important advantages and disadvantages. Suppose the problem domain, Ω is described by M nodes. Our purpose is to fit a function u by a linear combination of M shape functions γ_i, $i = 1, \ldots, M$, at any point of Ω such that:

$$u^h(\mathbf{r}) = \overset{=T}{\Gamma}(\mathbf{r})\bar{c} = \sum_{i=1}^{M} \gamma_i(\mathbf{r}) c_i, \mathbf{r} \in \Omega. \tag{3}$$

where u^h, $\overline{\overline{\Gamma}}$ and $\bar{c}$ are fitted value of u, shape function matrix and coefficient vector, respectively [31].

A. Approximants

When shape functions are approximants, $c_i \neq u^h(\mathbf{r}_i) \equiv u_i$. There are a number of methods for generating them, e.g., *Smoothed Particle Hydrodynamics* (SPH), *Reproducing Kernel Particle Method* (RKPM), and *Moving Least Square Methods* [31]. The most powerful and known method is MLS. There are two kinds of MLS methods; *conventional* and *matrix-free* [32]. While the generated shape functions from the conventional type are very accurate, the evaluation process involves numerous small size matrix computations. Moreover, vector implementation is not possible. Thus, for evaluating each shape function at n points, the routine should be executed n times, that makes it computationally inefficient. Furthermore, the computational complexity grows dramatically by increasing the order of partial derivatives. These complexities have motivated researchers to design matrix-free MLS methods. The simplest and historically the first of this kind is the *Shepard function* [33] which is fast and vectorizable. MLS shape functions have a valuable property that make them superior to interpolants in some applications; they are *localized* and nonzero only in a small portion of the problem domain.

B. Interpolants

For interpolants, $c_i = u^h(\mathbf{r}_i) \equiv u_i$. The methods for generating such functions are called *point interpolation methods* and have two main kinds; the older employs polynomials as bases functions and the newer one uses RBFs. The RBF based methods are superior because their moment matrix is guaranteed to be non-singular [31]. While, in general, approximants are more accurate, interpolants have three valuable features that make them preferable to approximants in some cases. First, they and their partial derivatives are easy to generate. Second, imposition of Dirichlet boundary condition is extremely simple, and third, vector implementation is possible. On the other hand, they suffer from a disadvantage; their evaluation involves working with large size matrices. In other words, they work well when they are *spread* over the entire problem domain [34].

IV. SELECTION OF MESHLESS SHAPE FUNCTIONS

This section is the most important part of the present paper. Improper selection of shape functions, especially in the case of IEs, can severely degrade the quality and efficiency of the numerical solution. Consider the first equation of (1) which we call the *differential part* with y as unknown. Based on the previous section, we expanded y over RBFs to expedite the analysis. Next, consider the second equation of (1), which we name the *integral part* with f as unknown. In this case, expanding over RBFs is not reasonable. Although this selection leads to a fast computation of shape functions, their distribution over the entire domain of the problem requires either a huge number of quadrature points or a background mesh for numerical integration. Another choice is the conventional MLS shape functions. This choice is also improper. While such functions are localized over a small portion of the problem domain, for numerical integration, many evaluations are needed and this considerably slows down the numerical solution. The best option seems to be the matrix-free MLS shape functions since they are localized and fast.

V. MESHLESS DISCRETIZATION

From a theoretical point of view, meshfree solution of (1) can be based on any of the Galerkin, Petrov-Galerkin and collocation methods. However, due to the complex nature of meshless shape functions, their evaluation is considerably time consuming. Consequently, Implementation of the first two choices may not be straightforward, since numerical integration involves numerous evaluations. Thus, only the collocation method is applied in this study. Here, discretization of (1) is performed by assuming scalar functions and operators. Generalization to vector case is straightforward.

Numerical solution of (1) by meshfree collocation method can be carried out by the following three steps. First, scatter M nodes over the problem domain and on its boundary. Second, expand the unknown functions over the proper meshfree shape functions, and third, equate both sides of the equation at the nodes and solve the corresponding linear system of equations after imposition of boundary conditions.

Following the aforementioned steps, let the problem domain Ω and the boundary $\partial\Omega$ be described by M nodes. Assume $\{\varphi_i\}_{i=1}^{M}$ and $\{\psi_i\}_{i=1}^{M}$ be sets of shape functions for the nodes, where φ_i and ψ_i represents the interpolant and approximant corresponding to the ith node, respectively. Following the previous section by expanding y over interpolants and f over approximants, i.e.:

$$\begin{cases} y^h(\mathbf{r}) = \boldsymbol{\Phi}^T(\mathbf{r})\cdot\hat{\mathbf{y}} = \sum_{i=1}^{M}\varphi_i(\mathbf{r})\widehat{y_i} \\ f^h(\mathbf{r}) = \boldsymbol{\Psi}^T(\mathbf{r})\cdot\hat{\mathbf{f}} = \sum_{i=1}^{M}\psi_i(\mathbf{r})\widehat{f_i} \end{cases}. \tag{4}$$

where y^h and f^h are interpolated and approximated value of y and f, respectively. Replacing the first Eq. of (4) into the first Eq. of (1) and collocating at the nodes leads to

$$\hat{\mathbf{e}} = \mathbf{K}_D\cdot\hat{\mathbf{y}}. \tag{5}$$

with

$$\begin{cases} \left[\hat{\mathbf{e}}\right]_p = e(\mathbf{r}_p) \\ \left[\mathbf{K}_D\right]_{pq} = O_D\left[\varphi_q(\mathbf{r}_p)\right] \end{cases}. \tag{6}$$

Similarly, by replacing the second Eq. of (4) into the second Eq. of (1),

$$\boldsymbol{\Phi}^T\cdot\hat{\mathbf{y}} = \mathbf{K}_I\cdot\hat{\mathbf{f}}. \tag{7}$$

where

$$\left[\mathbf{K}_I\right]_{pq} = O_I\left[\psi_q(\mathbf{r}_p)\right]. \tag{8}$$

What remains is imposition of the Dirichlet boundary condition that is the last equation of (1). Because this equation acts on f, we should first eliminate $\hat{\mathbf{y}}$ and relate the excitation vector $\hat{\mathbf{e}}$ to $\hat{\mathbf{f}}$, directly. Consequently:

$$\begin{cases} \hat{\mathbf{e}} = \mathbf{K}\cdot\hat{\mathbf{f}} \\ \mathbf{K} = \mathbf{K}_D\cdot\boldsymbol{\Phi}^{-T}\cdot\mathbf{K}_I \end{cases}. \tag{9}$$

The unknown coefficient vector $\hat{\mathbf{f}}$ can now be found by solving (9) after imposition of the boundary condition, which is now straightforward.

VI. GENERAL GUIDELINES FOR COMPUTING THE ENTRIES OF $\mathbf{K}_I$

The calculation of $\mathbf{K}_I$ is the most critical and time-consuming part of the final coefficient matrix, $\mathbf{K}$. This section provides guidelines for its accurate and efficient computation.

Numerical integration is a vital step in weighted residual methods. It can severely affect the accuracy and speed of the solution. In IE based methods, presence of the Green's function increases the complexity of this step, particularly for high order of singularities. Additionally, meshless shape functions are more complicated and their evaluation is considerably slower than elementary mathematical functions such as polynomials and complex exponentials. This becomes extremely visible, when numerical integration is involved in the analysis.

The key point of this section is noting that approximant shape functions are *bell-shaped* and consequently, can be well approximated by a single bell-shaped function such as Gaussian and Butterworth. As a 1D example:

$$\psi(x) \cong \begin{cases} a_G\exp\left(-\xi_G x^2\right), & \text{Gaussian} \\ a_B\left[1+\left(x/x_B\right)^{2n_B}\right]^{-1}, & \text{Butterworth} \end{cases}. \tag{10}$$

where the parameters a_G, ξ_G, a_B, x_B, and n_B can be easily estimated by curve fitting methods. A sample approximation of a 1D Shepard approximant is represented in Fig. 1.

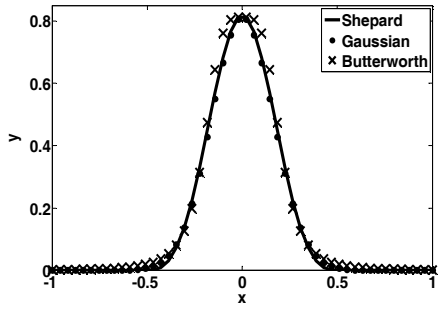

Fig. 1. Approximating a sample 1D Shepard approximant by Gaussian and Butterworth functions.

This simplifies handling of the problem and increases the computational efficiency. Moreover, since the Fourier transform of both Gaussian and Butterworth functions are available in all dimensions, such a substitution makes the understanding of the spectral behavior of the approximants possible. The importance of this point is made more comprehensible in the next section. The aforementioned matrix can be computed in both the space and the spectral domains. Thus, we split this section into two parts and discuss each case separately.

A. Space domain

In the space domain, some possible choices are *approximate Green's function*, *the Duffy transform* [35], *advanced quadratures* [36], *and fast convolution methods* [37]. Except for the last choice, all aforementioned methods are time consuming, but simple to implement. Although the method introduced in [37] is considerably more efficient than others, its implementation is not simple.

B. Spectral domain

Exploiting the spectral domain for computation of $\mathbf{K}_I$ is rooted in the convolutional nature of the EM IEs and can be performed in different ways. Considering (1) and (4), the mathematical form required for computing $\mathbf{K}_I$ is:

$$\begin{aligned} s &= \psi_i * G \\ &= \mathscr{F}^{-1}\left\{\mathscr{F}\left\{\psi_i\right\}\cdot\mathscr{F}\left\{G\right\}\right\}. \end{aligned} \tag{11}$$

where ψ_i is the approximant corresponding to the ith node and $\mathscr{F}$ stands for *continuous Fourier transform* (CFT). For this purpose, the most obvious choice is using the (inverse) fast Fourier transform, which can be efficiently computed by available FFT/IFFT algorithms. However, existence of singularity in the Green's function can potentially deteriorate the accuracy.

Here, we introduce our proposed method which is based on two assumptions. First, the problem domain and the boundary should be described by regular node arrangements. Under this assumption, all ψ_i approximants become shifted version of each other. The method can be potentially generalized to handle arbitrary configurations, which is currently under investigation. Second, it is necessary to approximate the approximants by a function having analytical Fourier transform. Under these assumptions, it is possible to compute (11) by a closed form expression. It is worth mentioning that this procedure is severely problem-dependent.

VII. NUMERICAL RESULTS

In this section, the guidelines are followed to solve five classic EM problems by the meshfree collocation method. Problem domains and boundaries are described by regular node arrangement for fast computation of the coefficient matrix. In all cases, d is the radial nodal distance. The approximant used is the Shepard function as defined by [33]:

$$\psi_i(\mathbf{r}) = w_i(\mathbf{r})\left(\sum_{j=1}^{M} w_j(\mathbf{r})\right)^{-1}. \tag{12}$$

with *quadric spline function* as its weighting defined by [38]:

$$w_i(\mathbf{r}) = w(d_i) = \begin{cases} 1-6d_i^2+8d_i^3-3d_i^4, & d_i \le r_0 \\ 0, & d_i > r_0 \end{cases}. \tag{13}$$

where M is the number of nodes, $d_i = |\mathbf{r}-\mathbf{r}_i|$ and r_0 is the *support size* of the Shepard function. For all 2D examples $r_0 = d/2^{1/2}$ is chosen. Approximants are approximated by a single Gaussian function for all cases. In addition, interpolants are constructed from *thin plate spline* (TPS) RBFs. Results are validated by convergence analysis [39]. Furthermore, convergence of the 1D dynamic case is compared with a pulse/rooftop MoM code and 2D dynamic cases are compared with RWG MoM codes developed by Makarov [40]. It should be pointed out that the number of nodes and unknowns are always denoted by M and N, respectively. Thus, for 1D and static examples N = M, whereas for 2D dynamic examples N = 2M. The error estimate is based on

$$r_e(u_m, u_{m+1}) = |u_{m+1}-u_m|/|u_m|. \tag{14}$$

with u_m being a functional of the field variable computed at the mth pass. Finally, the simulations are executed on a Intel(R) Core(TM)2 6700 CPU with 4 GB RAM.

A. Static charge over infinite PEC strip

As a 1D scalar static IE, consider the equation governing the static charge distribution over a 2 m width PEC infinite strip [27]:

$$\begin{cases} \int_{-1}^{1} G(x-x')\,q_s(x')\,dx' = 1, & |x| \le 1 \\ G(x) = -(2\pi\varepsilon_0)^{-1}\ln|x| \end{cases}. \tag{15}$$

It is assumed that the strip has the potential of 1 V and is placed on the x-y plane, along the y-axis and is centered at the origin. By comparing (15) with (1) one can recognize that:

$$\begin{cases} e = 1 \\ f = q_s(x) \\ O_D(u) = u \\ \Omega : -1 \le x \le 1 \end{cases}. \tag{16}$$

Thus, the problem has neither the differential part nor the boundary condition. For this problem $r_0 = 1.5d$ and adaptive Gauss-Kronrod quadrature is used for numerical integrations. The convergence curve in the sense of total charge and the normalized charge distribution across the strip are depicted in Fig. 2.

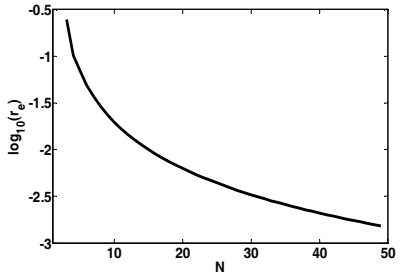

(a)

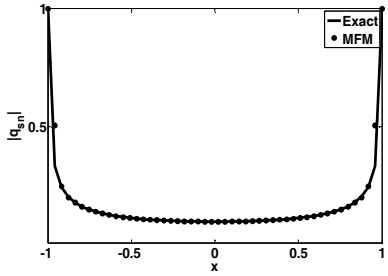

(b)

Fig. 2. Static charge per unit length on an infinite PEC strip: (a) convergence curve, (b) spatial distribution of normalized charge.

B. Static charge density over square PEC plate

As a 2D scalar static IE, consider the equation governing the static charge density distribution over a unit length square PEC plate [25]:

$$\begin{cases} \int_{Plate} G(\mathbf{r}-\mathbf{r}')\rho_s(\mathbf{r}')d\mathbf{r}' = 1, |x| \wedge |y| \le 1 \\ G(\mathbf{r}) = (4\pi\varepsilon_0 r)^{-1} \end{cases}. \quad (17)$$

It is assumed that the plate has the potential of 1 V and is placed on the x-y plane, centered at the origin. By comparing (17) with (1), a similar expressions to (16) can be written. Thus, problem has neither the differential part nor boundary condition. Following the proposed method, the computation of the $\mathbf{K}_I$ matrix can be carried out without numerical integration by noting that

$$\begin{cases} \mathcal{F}\{\exp(-\xi r^2)\} = (\pi/\xi)\exp(-k_r^2/4\xi) \\ \mathcal{F}\{G\} = k_r^{-1} \end{cases}. \quad (18)$$

where $r = (x^2 + y^2)^{1/2}$. Therefore [41]:

$$\begin{aligned} s(r) &= (\pi/\xi)\int_0^\infty \exp(-k_r^2/4\xi)k_r^{-1}J_0(k_r r)k_r dk_r \\ &= (\pi/4\xi)^{1/2}\exp(-\xi r^2/2)I_0(\xi r^2/2). \end{aligned} \quad (19)$$

The convergence curve in the sense of capacity per unit length and the normalized charge density distribution over the plate are depicted in Figs. 3(a) and 3(b), respectively. In addition, Fig. 3(c) compares the computational cost of $\mathbf{K}_I$ by direct numerical integration in the space domain and the proposed spectral domain method based on (19).

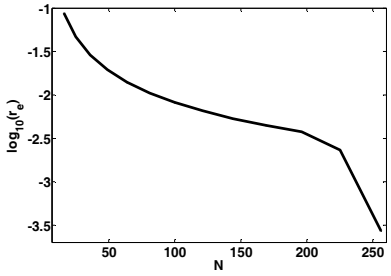

(a)

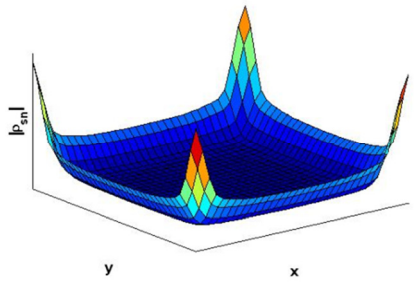

(b)

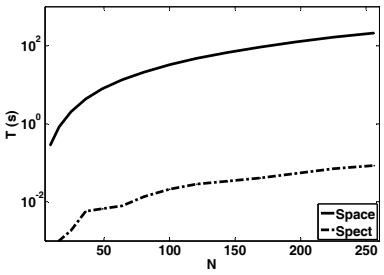

(c)

Fig. 3. Static charge density over square PEC plate: (a) convergence curve, (b) spatial distribution of normalized charge density, (c) computation cost of $\mathbf{K}_I$.

C. Scattering by a thin PEC wire

As a 1D scalar dynamic IE, consider the equation governing the current distribution over a 6λ thin PEC wire. The problem can be formulated by two mathematically equivalent IEs, i.e., EFIE and MPIE [25], [42]:

$$\begin{cases} EFIE: j\omega\left(1+k_0^{-2}\,\partial^2/\partial z^2\right)A=1 \\ MPIE: j\omega A+\nabla V=1 \end{cases}, |z|<3\lambda. \tag{20}$$

subject to:

$$I=0, |z|=3\lambda. \tag{21}$$

where

$$\begin{cases} A(z)=\mu_0\int\limits_{Wire} G(z-z')I(z')dz' \\ V(z)=-(j\omega\varepsilon_0)^{-1}\int\limits_{Wire} G(z-z')\dfrac{dI(z')}{dz'}dz' \end{cases}. \tag{22}$$

and

$$G(z)=\left(4\pi\sqrt{z^2+a^2}\right)^{-1}\exp\left(-jk\sqrt{z^2+a^2}\right). \tag{23}$$

The wire is placed on the *z*-axis, centered at the origin, with radius $a = 0.00628\lambda$. It is assumed that the wire is normally illuminated by an incident plane wave of unit amplitude and angular frequency of ω. By comparing (20)-(23) with (1),

$$\begin{cases} e=1 \\ f=I(z) \\ O_D(u)=j\omega\left(1+k_0^{-2}\,\partial^2/\partial z^2\right)u. \\ \Omega: -3\lambda<z<3\lambda \\ \partial\Omega: z=\pm 3\lambda \end{cases} \tag{24}$$

Thus, both formulations have differential part and boundary condition. In this case, $r_0 = 2.5d$ and adaptive Gauss-Kronrod quadrature is used for numerical integrations. The convergence curves in the sense of normalized monostatic RCS and the normalized current distribution for 35 nodes and reconstructed at 200 nodes are depicted in Figs. 4(a) and 4(b), respectively. Additionally, Fig. 4(c) compares the computational cost of $\mathbf{K}_I$ by direct numerical integration in the space with the proposed method exploiting FFT.

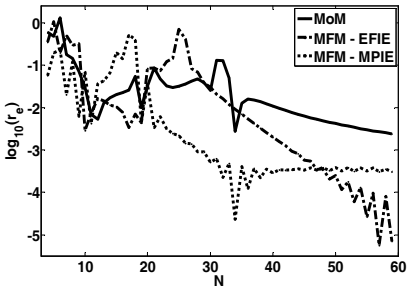

(a)

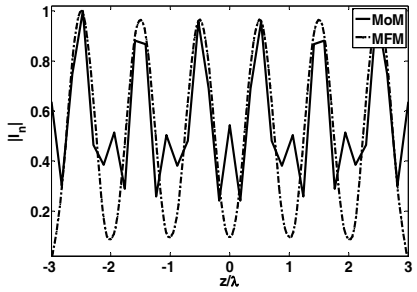

(b)

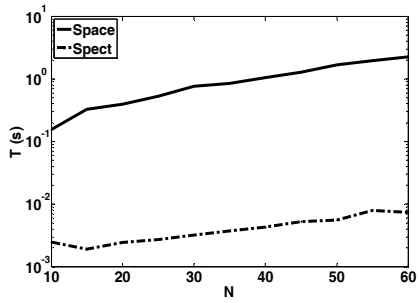

(c)

Fig. 4. Scattering by a 6λ thin PEC wire: (a) convergence curves, (b) spatial distribution of normalized current for 35 nodes and reconstructed at 200 nodes, (c) computation cost of $\mathbf{K}_I$.

D. Scattering by a PEC square plate

As a 2D vector dynamic IE, consider the equation governing the current density distribution over a 3λ PEC square plate. Similar to the previous case, the problem can be formulated by EFIE and MPIE:

$$\begin{cases} EFIE: j\omega\left(1+k_0^{-2}\nabla\nabla\cdot\right)\mathbf{A}=\hat{\mathbf{x}} \\ MPIE: j\omega\mathbf{A}+\nabla V=\hat{\mathbf{x}} \end{cases}, |x|\wedge|y|<3\lambda/2. \tag{25}$$

subject to:

$$\begin{cases} J_x=0, |x|=3\lambda/2 \\ J_y=0, |y|=3\lambda/2 \end{cases}. \tag{26}$$

where:

$$\begin{cases} \mathbf{A}(\mathbf{r})=\mu_0\int\limits_{Plate} G(\mathbf{r}-\mathbf{r}')\mathbf{J}(\mathbf{r}')d\mathbf{r}' \\ V(\mathbf{r})=-(j\omega\varepsilon_0)^{-1}\int\limits_{Plate} G(\mathbf{r}-\mathbf{r}')\nabla'\cdot\mathbf{J}(\mathbf{r}')d\mathbf{r}' \end{cases}. \tag{27}$$

and:

$$G(\mathbf{r})=(4\pi r)^{-1}\exp(-jkr). \tag{28}$$

The plate is placed on the *x*-*y* plane, centered at the origin and illuminated by an incident wave with an *x*-directed electric field of unit amplitude

and angular frequency of ω. Comparing (25)-(28) with (1) leads to

$$\begin{cases} e = \mathbf{x} \\ f = \mathbf{J}(\mathbf{r}) \\ O_D(u) = j\omega\left(1 + k_0^{-2}\nabla\nabla\cdot\right)u \\ \Omega : -3\lambda/2 < x,\, y < 3\lambda/2 \\ \partial\Omega : (x,\, y) = (\pm 3\lambda/2,\, \pm 3\lambda/2) \end{cases} . \tag{29}$$

As in the previous case, both formulations have differential part and boundary condition. By applying the proposed spectral method, it is straightforward to show that the mathematical forms of the integrals for computing $\mathbf{K}_I$ are

$$\begin{cases} g_1(r) = \int_0^\infty (jk_z)^{-1}\,\widetilde{\psi}(r) J_0(k_r r) k_r dk_r \\ g_2(r) = \cos\theta \int_0^\infty (jk_z)^{-1}\,\widetilde{\psi}(r) J_1(k_r r) k_r^2 dk_r \\ g_3(r) = \sin\theta \int_0^\infty (jk_z)^{-1}\,\widetilde{\psi}(r) J_1(k_r r) k_r^2 dk_r \end{cases} . \tag{30}$$

where $\tan(\theta) = y/x$, and:

$$\begin{cases} \widetilde{\psi}(r) = \mathcal{F}\{\psi(r)\} = e^{-\frac{k_r^2}{4\xi}} \\ \widetilde{G}(r) = \mathcal{F}\{G(r)\} = (jk_z)^{-1} = \left(k_r^2 - k_0^2\right)^{-1/2} \end{cases} . \tag{31}$$

For fast evaluation of (31), we follow the idea behind the *discrete complex image method* (DCIM) [43]. Suppose:

$$\widetilde{\psi}(r) = \sum_{m=1}^{M} a_m e^{-b_m k_z} . \tag{32}$$

which can be efficiently calculated by the *matrix-pencil-method* (MPM) [44]. Now, a closed-form of the aforementioned integrals can be readily obtained by making use of the *Sommerfeld identity* and its first derivative [45]. The convergence curves in the sense of normalized monostatic RCS and the normalized current density distribution for N = 2×19×19 and reconstructed at 22500 nodes are depicted in Figs. 5(a) and 5(b), respectively. Additionally, the computational cost of $\mathbf{K}_I$ is reported in Fig. 5(c).

E. Scattering by a PEC circular plate

As 2D vector dynamic IE over a non-rectangular domain, consider the equation governing the current density distribution over a PEC circular plate with $\lambda/4$ radius. Similar to the previous case, the problem can be formulated by EFIE and MPIE, subject to

$$J_x \cos\theta + J_y \sin\theta = 0,\; x^2 + y^2 = (\lambda/4)^2 . \tag{33}$$

The plate is placed on the *x*-*y* plane, centered at the origin. The excitation, discretization parameters and numerical integration strategy are the same as the previous problem. The convergence curves in the sense of normalized monostatic RCS, a nodal arrangement based on 98 nodes and the corresponding normalized current density distribution reconstructed at 17500 nodes, are depicted in Fig. 6.

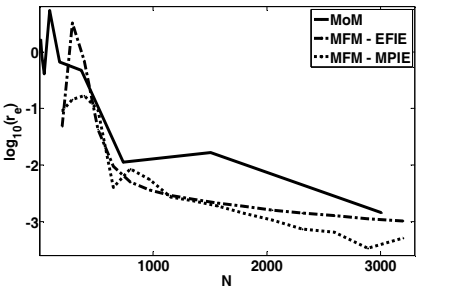

(a)

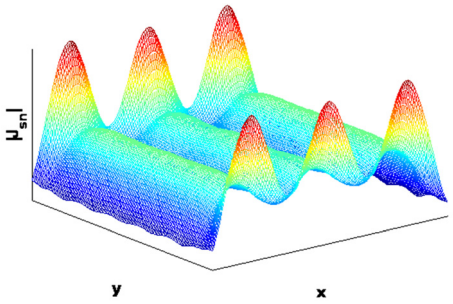

(b)

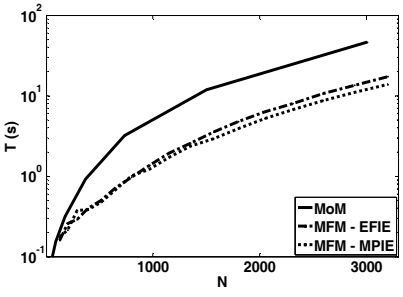

(c)

Fig. 5. Scattering by a 3λ PEC square plate: (a) convergence curves, (b) spatial distribution of normalized current density for N = 2×19×19, (c) computation cost of $\mathbf{K}_I$.

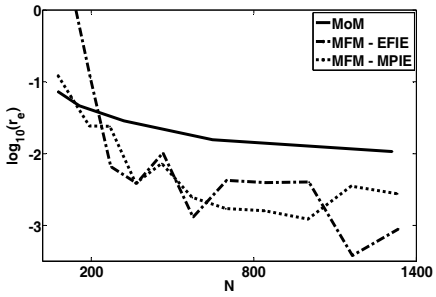

(a)

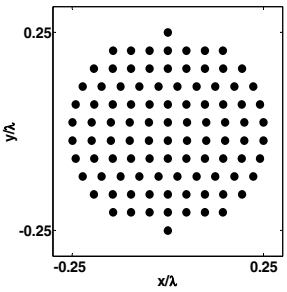

(b)

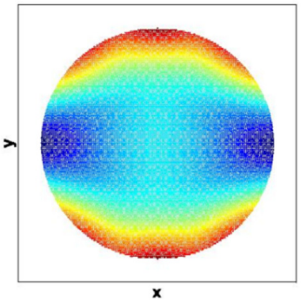

(c)

Fig. 6. Scattering by a PEC circular plate with $\lambda/4$ radius: (a) convergence curves, (b) nodal arrangement based on 98 nodes, (c) reconstructed solution at 17500 nodes.

VIII. CONCLUSION

The meshfree collocation method is formulated for numerical solution of electromagnetic integral equations including EFIE and MPIE. Both RBF interpolants and Shepard approximants are utilized for efficient analysis. Suggestions are also made for bypassing numerical integration.

ACKNOWLEDGMENT

The authors acknowledge Prof. M. Dehghan for inputs in meshfree methods, and Prof. R. F. Dana, for inputs in validation techniques.

REFERENCES

[1] Y. Marechal, "Some Meshless Methods for Electromagnetic Field Computations," *IEEE Trans. Magn*., vol. 34, no. 5, pp. 3351-3354, 1998.

[2] C. Herault and Y. Marechal, "Boundary and Interface Conditions in Meshless Methods," *IEEE Trans. Magn.*, vol. 35, no. 3, pp. 1450-1453, 1999.

[3] S. L. Ho, S. Yang, J. M. Machado, and H. C. Wong, "Application of a Meshless Method in Electromagnetics," *IEEE Trans. Magn.*, vol. 37, no. 5, pp. 3198-3201, 2001.

[4] L. Xuan, Z. Zeng, B. Shanker, and L. Udpa, "Meshless Method for Numerical Modeling of Pulsed Eddy Currents," *IEEE Trans. Magn*., vol. 40, no. 6, pp. 3457-3462, 2004.

[5] S. L. Ho, S. S. Yang, H. C. Wong, and G. Ni, "Meshless Collocation Method based on Radial Basis Functions and Wavelets," *IEEE Trans. Magn.*, vol. 40, no. 2, pp. 1021-1024, 2004.

[6] S. L. Ho, S. S. Yang, G. Ni , H. C. Wong, and Y. Wang, "Numerical Analysis of Thin Skin Depths of 3-D Eddy-Current Problems using a Combination of Finite Element and Meshless Methods," *IEEE Trans. Magn*., vol. 40, no. 2, pp. 1354-1357, 2004.

[7] S. L. Ho, S. S. Yang, H. C. Wong, E. W. C. Lo and G. Ni, "Refinement Computations of Electromagnetic Fields using FE and Meshless Methods," *IEEE Trans. Magn*., vol. 41, no. 5, pp. 1456-1459, 2005.

[8] Y. Zhang, K. R. Shao, D. X. Xie and J. D. Lavers, "Meshless Method based on Orthogonal Basis for Electromagnetics," *IEEE Trans. Magn*., vol. 41, no. 5, pp. 1432-1435, 2005.

[9] Q. Li and K. Lee, "Adaptive Meshless Method for Magnetic Field Computation," *IEEE Trans. Magn*., vol. 42, no. 8, pp. 1996-2003, 2006.

[10] R. K. Gordon, W. E. Hutchcraft, "The Use of Multiquadric Radial Basis Functions in Open Region Problems," *Applied Computational Electromagnetics Society (ACES) Journal*, vol. 21, no. 2, pp. 127-134, July 2006.

[11] Y. Zhang, K. R. Shao, J. Zhu, D. X. Xie and J. D. Lavers, "A Comparison of Point Interpolative Boundary Meshless Method based on PBF and RBF for Transient Eddy-Current Analysis," *IEEE Trans. Magn*., vol. 43, no. 4, pp. 1497-1500, 2007.

[12] F. G. Guimaraes, R. R. Saldanha, R. C. Mesquita, D. A. Lowther, and J. A. Ramirez, "A Meshless Method for Electromagnetic Field Computation based on the Multiquadratic Technique," *IEEE Trans. Magn.*, vol. 43, no. 4, pp. 1281-1284, 2007.

[13] S. Ikuno, K. Takakura, and A. Kamitani, "Influence of Method for Imposing Essential Boundary Condition on Meshless Galerkin/Petrov-Galerkin Approaches," *IEEE Trans. Magn*., vol. 43, no. 4, pp. 1501-1504, 2007.

[14] S. McFee, D. Ma, and M. Golshayan, "A Parallel Meshless Formulation for h-p Adaptive Finite

Element Analysis," *IEEE Trans. Magn*., vol. 44, no. 6, pp. 786-789, 2008.

[15] T. Kaufmann, C. Fumeaux, R. Vahldieck, "The Meshless Radial Point Interpolation Method for Time-Domain Electromagnetics", *IEEE MTT-S Int. Microwave Symp. Dig.*, Atlanta, pp. 61 - 64, 2008.

[16] Y. Yu and Z. Chen, "A 3-D Radial Point Interpolation Method for Meshless Time-Domain Modeling," *IEEE Trans. Microwave Theory Tech.*, vol. 57, no. 8, pp. 2015-202, 2009.

[17] Y. Yu and Z. Chen, "Towards the Development of an Unconditionally Stable Time-Domain Meshless Method," *IEEE Trans. Microwave Theory Tech.*, vol. 58, no. 3, pp. 578- 586, 2010.

[18] T. Kaufmann, C. Engström, C. Fumeaux, R. Vahldieck, "Eigenvalue Analysis and Longtime Stability of Resonant Structures for the Meshless Radial Point Interpolation Method in Time Domain", *IEEE Trans. Microwave Theory Tech.*, vol. 58, no. 12, pp. 3399 - 3408, 2010.

[19] R. D. Soares, R. C. Mesquita, F. J. S. Moreira, "Axisymmetric Electromagnetic Resonant Cavity Solution by a Meshless Local Petrov-Galerkin Method," *Applied Computational Electromagnetics Society (ACES) Journal*, vol. 26, no. 10, pp. 792-799, October 2011.

[20] M. Zhang, L. Lingxia, P. Zhou, and X. Zhang, "A Novel Mesh-Free Method for Electromagnetic Scattering from a Wire Structure," *PIERS Online*, vol. 3, no. 6, pp. 774-776, 2007.

[21] D. Mirzaei and M. Dehghan, "A Meshless based Method for Solution of Integral Equations," *Appl. Numer. Math.*, vol. 60, no. 3, pp. 245-262, 2010.

[22] W. L. Nicomedes, R. C. Mesquita, and F. J. S. Moreira, "An Integral Meshless-based Approach in Electromagnetic Scattering," *COMPEL Int. J. Comput. Math. Elec. Elec. Eng.*, vol. 29, no. 6, pp. 1464-1473, 2010.

[23] S. J. Lai, B. Z. Wang , and Y. Duan, "Meshless Radial Basis Functions Method for Solving Hallen's Integral Equation," *Applied Computational Electromagnetic Society (ACES) Journal*, vol. 27, no. 1, pp. 9-13, 2012.

[24] W. C. Chew, *Waves and Fields in Inhomogeneous Media*. IEEE Press, 1995.

[25] R. F. Harrington, *Field Computation by Moment Methods*. New York: Macmillan, 1968.

[26] J. R. Mosig, "Arbitrary Shaped Microstrip Structures and their Analysis with a Mixed Potential Integral Equation," *IEEE Trans. Microwave Theory Tech.*, vol. 36, no. 2, pp. 314-323, 1988.

[27] R. Bancroft, *Understanding Electromagnetic Scattering Using the Moment Method*. Artech House, 1996.

[28] J. Jin and J. L. Volakis, "A Finite Element-Boundary Integral Formulation for Scattering by Three-Dimensional Cavity-Backed Apertures," *IEEE Trans. Antennas Propagat.*, vol. 39, no. 1, pp. 97-104, 1991.

[29] Z. Huang, K. R. Demarest, and R. G. Plumb, "An FDTD/MoM Hybrid Technique for Modeling Complex Antennas in the Presence of Heterogeneous Grounds," *IEEE Trans. Geosci. Remote*, vol. 37, no. 6, pp. 2692-2698, 1999.

[30] B. Honarbakhsh and A. Tavakoli, "Scattering by a 2D Crack: The Meshfree Collocation Approach," *Applied Computational Electromagnetic Society (ACES) Journal*, vol. 27, no. 3, pp. 278-284, 2012.

[31] G. R. Liu, *Mesh Free Methods*. CRC Press, 2003.

[32] G. E. Fasshauer, *Approximation Theory X: Wavelets, Splines and Applications*. Vanderbilt University Press, 2002.

[33] D. Shepard, "A Two Dimensional Interpolation Function for Irregularly Spaced Data," in *Proc. 23rd Nat. Conf. ACM*, pp. 517–523, 1968.

[34] R. Schaback, "Limit Problems for Interpolation by Analytic Radial Base Functions," *Comp. Appl. Math.*, vol. 212, no. 2, pp. 127-149, 2008.

[35] M. G. Duffy, "Quadrature over a Pyramid or Cube of Integrands with a Singularity at a Vertex," *SIAM J. Numer. Anal.*, vol. 19, pp. 1260-1262, 1982.

[36] L. F. Shampine, "Vectorized Adaptive Quadrature in MATLAB," *J. Comput. Appl. Math.*, vol. 211, pp. 131-140, 2008.

[37] G. Beylkin, C. Kurcz and L. Monzon, "Fast Convolution with the Free Space Helmholtz Green's Function," *J. Comput. Phys.*, vol. 228, pp. 2770-2791, 2009.

[38] G. R. Liu and Y. T. Gu, *An Introduction to MeshFree Methods and Their Programming*. Springer, 2005.

[39] J. C. Rautio, "The Microwava Point of View on Software Validation," *IEEE Antennas Propagat. Mag*., vol. 38, no. 2, pp. 68-71, 1996.

[40] S. N. Makarov, *Antenna and EM Modeling with MATLAB*, Wiley-InterScience, 2002.

[41] I. S. Gradshteyn, I. M. Ryzhik, A. Jeffrey, and D. Zwillinger, *Table of Integrals, Series, and Products*, 6th Edition, Academic Press, 2000.

[42] W. C. Gibson, *The Method of Moments in Electromagnetics*. Chapman & Hall/CRC, Taylor & Francis Group, 2008.

[43] Y. L. Chow, J. J. Yang, D.G. Fang, G. E. Howard, "A Closed-Form Green's Function for the Thick Microstrip Substrate," *IEEE Trans. Microwave Theory Tech.*, vol. 39, no. 3, pp. 588-592, 1991.

[44] T. K. Sarkar, O. Pereira, "Using the Matrix Pencil Method to Estimate the Parameters of a Sum of Complex Exponentials," *IEEE Antennas Propagat. Mag*., vol. 37, no. 3, pp. 48-55, 1995.

[45] M. Yuan, T. K. Sarkar, M. Salazar-Palma, "A Direct Discrete Complex Image Method from the Closed-Form Green's Functions in Multilayered Media" *IEEE Trans. Microwave Theory Tech*., vol. 54, no. 3, pp. 1025-32, 2006.

Babak Honarbakhsh was born in Tehran, Iran. He received his B.S. and M.S. degrees in electrical engineering from Amirkabir University of Technology where he is currently working toward his Ph.D. degree. His current research interest is numerical solution of electromagnetic problems by meshfree methods.

Ahad Tavakoli was born in Tehran, Iran, on March 8, 1959. He received B.S. and M.S. degrees from the University of Kansas, Lawrence, and the Ph.D. degree from the University of Michigan, Ann Arbor, all in electrical engineering, in 1982, 1984, and 1991, respectively.

He is currently a Professor in the Department of Electrical Engineering at Amirkabir University of Technology. His research interests include EMC, scattering of electromagnetic waves and microstrip antennas.